euspen's 22nd International Conference & Exhibition, Geneva, CH, May/June 2022

www.euspen.eu

Alleviating stress concentrations by constant curvature flexure mechanisms

J.J. de Jong[1], D.M. Brouwer[1]

[1]*University of Twente, Enschede, The Netherlands, Precision Engineering Lab*

j.j.dejong@utwente.nl

Abstract

In high precision applications flexures are used to accurately guide motion. Here it is essential to obtain sufficient off-axis support stiffness as to mitigate parasitic dynamics. When deflecting, stress concentrations limit the flexure thickness and hence the support stiffness and loadability of the structure. In this paper we present an approach to make the curvature and stress constant over the flexure such that its thickness and consequently its support-stiffness may be increased. We show this approach with a *DiamondFlex* element. This DiamondFlex structure supports the endpoint forces such that the guiding flexure only experiences a bending moment, which results in a constant curvature and stress over the length of the flexure. Application of this approach to a parallel flexure guidance enables a thickness increase of $45\ \%$, increasing the support stiffness by a factor 2.5.

Keywords: Flexure mechanisms, Constant curvature, Optimization, Precision engineering

1. Introduction

Flexure mechanisms guide motion with virtually no play, backlash or wear [1]. Therefore, these mechanisms provide highly predictable motion, well-suited for high-precision applications. However, the stroke of flexure mechanisms is limited due to stress concentrations that occur due to deflection.

In pursuit of large stroke flexure mechanisms, several solutions have been proposed to homogenize the stress over the flexures, including elliptical notch hinges [2], [3], tapered flexures [4], and pre-curved flexures [5]. Alternatively, the support stiffness may be retained for large stroke by serial and parallel connection of multiple flexural elements [6]. Such approaches rely on systematically adding and rearranging known flexural building blocks to optimize for a particular load case. As such, it is desired to have a full and characterized inventory of available flexural elements.

In this study, we propose a new constant curvature flexural building block, the DiamondFlex (Figure 1). This alleviates stress concentrations in a guiding leaf spring by carrying the out-of-plane forces by folded leaf springs (FLS). This way the guiding leaf spring only experiences a pure bending moment leading to a homogenous stress distribution over the length of the flexure (Figure 2). This flexure arrangement may be used as a structural element to replace leaf springs with high stress concentrations to enable ticker leaf springs for a higher support stiffness of flexure mechanisms. The usefulness of the proposed flexural element is shown on a parallel flexure guide.

2. Method

To show the proposed method, first the basic principles of stress elevation through constant curvature mechanisms are treated (2.1), followed by details of the DiamondFlex (2.2) and the application to a parallel flexure guide (2.3).

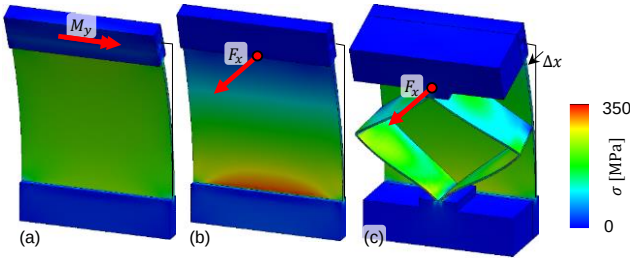

Figure 1. (*a*) When a leaf spring is loaded by a pure moment, its curvature and stress is constant along the length of the leaf spring. (*b*) When the leaf spring is subjected to an endpoint force, stress concentrations occur at the base due to the higher moments near the fixture. (*c*) The *DiamondFlex* consist of two additional folded leaf springs that carry the out-of-plane forces such that the main leaf spring is again subjected to a pure moment and stress concentrations are avoided. All cases are loaded to reach $\Delta x = 15$ mm deflection.

2.1 *The principle of constant curvature flexure mechanisms*

To illustrate the advantages of having a constant curvature over the flexure we consider two load cases: a flexure that is loaded 1) by a pure moment and 2) by an endpoint force to reach a given angle or translation.

The curvature $\phi'(s)$ of bending flexures at distance s along the elastic line, is proportional to the internal bending moment $M(s)$ and the stress σ_b

$$M(s) = EI\phi'(s), \qquad \sigma_b(s) = \frac{t}{2I}M(s) \tag{1}$$

where t, l, I, and E are the flexure thickness, length, moment of inertia and Youngs Modulus, respectively.

For flexures under a pure bending moment M, the maximal bending stress σ_b, deflection angle ϕ and displacement Δx are given by

$$\sigma_b = \frac{1}{2}\frac{t}{I}M, \qquad \phi = \frac{l}{EI}M, \qquad \Delta x = \frac{1}{2}\frac{l^2}{EI}M \tag{2}$$

When a flexure is loaded by an endpoint force F these quantities become

$$\sigma_b = \frac{1}{2}\frac{tl}{I}F, \qquad \phi = \frac{1}{2}\frac{l^2}{EI}F, \qquad \Delta x = \frac{1}{3}\frac{l^3}{EI}F \tag{3}$$

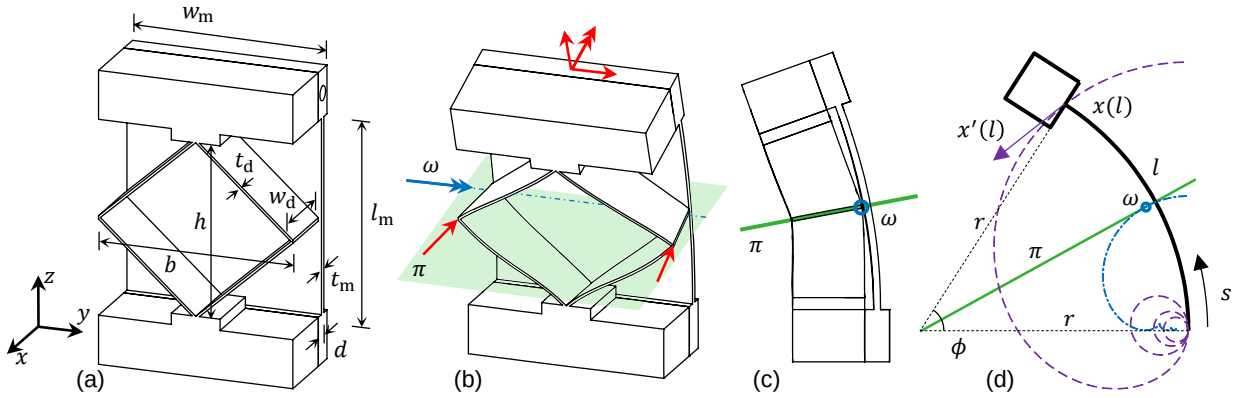

Figure 2. The anatomy of the *DiamondFlex* in undeformed (a) and deformed state (b, c). A main guiding leaf spring is supported by two folded leaf springs (FLS). Since the main leaf spring has 3 constraints (indicated by red arrows) and the FLSs constrain one translation each, the remaining DOF is a rotation around the common intersecting line ω, which lies on the plane of symmetry π. (d) When a constant curvature flexure is deflected, its endpoint $x(l)$ follows a spiraling curve (purple).

The main difference between the force and a moment load case is that the latter results in a uniform stress distribution over the flexure as the internal moment is constant over its length, whereas the latter case results in stress concentrations at the base, where the internal moment is maximal (Fig 1.a, b).

To prevent exceeding a given stress maximum $\sigma_{\max}$ (e.g., to avoid yield or fatigue), the thickness should be limited for a given deflection angle. For the two load cases we obtain a maximum thickness of

$$t_{\mathrm{F},\phi} = \sigma_{\max}\frac{l}{E}\frac{1}{\phi}, \qquad t_{\mathrm{M},\phi} = 2\sigma_{\max}\frac{l}{E}\frac{1}{\phi} = 2t_{\mathrm{F},\phi} \tag{4}$$

Here we can see that maximum thickness for the moment load case $t_{\mathrm{M},\phi}$ is double that of the force load case $t_{\mathrm{F},\phi}$, allowing a higher support stiffness. Similarly, when we desire a particular displacement, we see a 50 % increase in maximum thickness when comparing the moment to the force load case.

$$t_{\mathrm{F},\Delta x} = \frac{2}{3}\sigma_{\max}\frac{l^2}{E}\frac{1}{\Delta x}, \qquad t_{\mathrm{M},\Delta x} = \sigma_{\max}\frac{l^2}{E}\frac{1}{\Delta x} = \frac{3}{2}t_{\mathrm{F},\Delta x} \tag{5}$$

For small deflections we can expect a support-stiffness proportional to the thickness of the flexures while the driving force is affected by cube of the thickness. For large deflections however, the flexure thickness has a stronger influence on the support stiffness. For such cases it is especially advantageous to maximize the flexure thickness by making the curvature and stress more uniform over the length of the flexure.

2.2 DiamondFlex

2.2.1 Anatomy of the DiamondFlex

In this paper we present a flexural building block, the DiamondFlex, that induces a constant curvature in a 'main flexure' even when loaded by an endpoint force (Fig 1.c). The DiamondFlex consist of two folded leaf springs that are arranged alongside this main flexure (Fig 2). Each folded leaf spring constrains a pure translation along its fold line such that, combined, they constrain torsion along the longitudinal direction and parallel translation of the flexure tip.

Together with the constraints imposed by the main flexure, we are left with a pure bending motion about a rotation axis. Initially, this rotation axis is along the line that intersect the main flexure and both fold lines of the FLSs.

An alternative interpretation for the function of the DiamondFlex is that the actuation force is decomposed in a bending moment and a pure force passing through the plane of the fold lines. The FLSs carry the pure force, while the main flexure only experiences a pure bending moment with a constant stress over its length.

The design parameters are shown in Figure 2 and Table 1.

2.2.2 Kinematics of the DiamondFlex

We study the motion of the DiamondFlex first by assuming a perfect constant curvature motion of the main flexure. This allows us to choose design parameters to avoid internal collision (interference).

When this main flexure is subject to a pure moment its elastic line (Fig 2.c) follows an arc

$$x(s) = r\left(\begin{bmatrix}1\\0\end{bmatrix} + \begin{bmatrix}-\cos(\phi s)\\ \sin(\phi s)\end{bmatrix}\right), \quad s = 0 \dots 1 \tag{6}$$

Where $r = l/\phi$ is the radius of curvature. The tip of the flexure therefore moves over a spiraling path. From this it can be computed that the distance from the center of curvature to the instantaneous center of rotation is $r/|\phi|$, indicating that the instantaneous center of rotation p does not stay on the elastic line but moves inwards with larger bending angles.

To avoid interference, a sufficient separation distance d (Fig 2.a) between the guiding flexure and two FLSs is needed. To estimate the minimal separation, we use a first order approximation and assume leaf springs of the FLS purely twist about the edge closed to main flexure. These edges therefore remain rather straight, and we may approximate that interference occurs when

$$d = r - \sqrt{r^2 - l^2/4} \tag{7}$$

2.2.3 Statics of DiamondFlex

Although the Diamond structure lowers the stresses of the main flexure, large stresses typically occur in the FLSs of the Diamond. These stresses can be attributed to a combination of 1) torsion along the longitudinal axes of the FLS flexures, 2) an

Table 1. The design parameter of the main flexure and the DiamondFlex as used in the parallel flexure guidance

	Symbol	PFG base-line values	Unit
Displacement	Δx	5.00	mm
Stress maximum	$\sigma_{\max}$	350	MPa
Elastic modulus	E	210	GPa
Shear modulus	G	70.0	GPa
Guidance width	a	150	mm
Main length	l_m	100	mm
Main width	w_m	50.0	mm
Main thickness	t_m	1.11	mm
Diamond thickness	t_d	0.40	mm
Diamond width	w_d	22.5	mm
Diamond height	h	50.0	mm
Diamond breadth	b	50.0	mm
Separation distance	d	1.25	mm

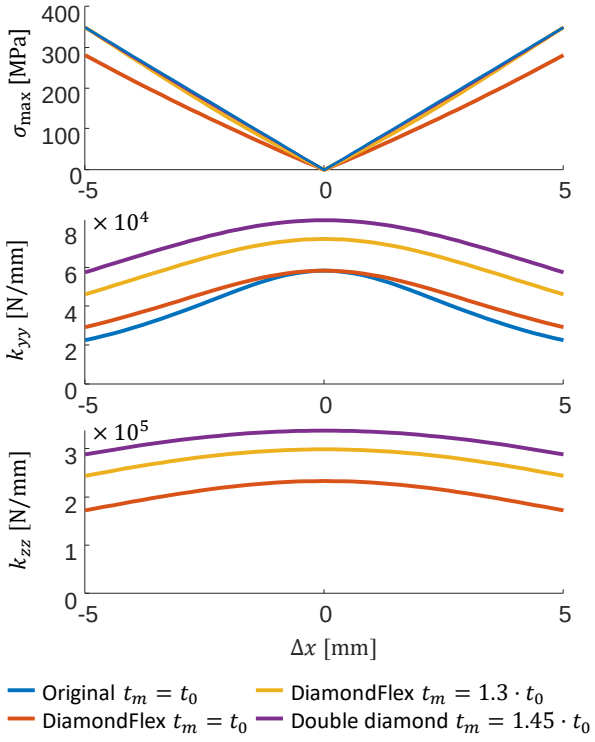

Figure 3. The maximal stress in the parallel flexure (*top*), lateral support stiffness (*middle*) and vertical support stiffness over deflection (*bottom*). Here the results of the original flexure (blue), DiamondFlex with original flexure thickness (red), DiamondFlex with increased flexure thickness (yellow), and double DiamondFlex with increased flexure thickness (purple) are shown.

out-of-plane bending, and 3) an in-plane loading due to driving force.

This combined load case leads to a trade-off in the width w_d and thickness t_d of the flexure. Wide and thick flexures reduce the stress due the in-plane loads but also increase the stress due to torsion and out-of-plane bending.

Currently, we do not have an accurate analytic model of the stresses to find an optimal trade-off. Therefore, we rely on a flexible multibody simulation software [7] in conjunction with optimization to find suitable designs.

2.2.4 Double diamond

To increase the load carrying capabilities of the FLS flexures a Diamond on both sides of the main flexure can be considered. The actuation force is then carried by more flexures, reducing the maximum stress in the FLSs such that the main flexure can be made ticker.

2.3 Case study: application to a parallel flexure guide

To show that this DiamondFlex element may aid flexure mechanisms we apply the proposed strategy to a parallel flexure guide. This flexure guide is designed to support a linear motion of $\Delta x = +/- 5$ mm. Since both ends of the flexures are constrained to a pure translation, stress concentrations occur at these fixtures. To alleviate these stress concentrations, we use two DiamondFlex elements per flexure

We evaluate four cases: 1) baseline consisting of only the main flexures, 2) adding the DiamondFlex with while retaining the original main flexure thickness, 3) adding DiamondFlex with increased main flexure thickness and 4) adding a double DiamondFlex. In the latter two cases we maximized the main flexure thickness until the maximum stress equaled that of the original case. Here we optimized the width $(w_\mathrm{d})$of the FLS while fixing the breadth b and height h of the DiamondFlex to the length l_m and width w_m of the main flexure and the FLS thickness t_d to the minimal producible value. The corresponding values can be found in Tables 1 and 2.

3. Case study results: application to a parallel flexure guide

Figure 3 shows the simulation results, whereas Figure 4 shows the stress distribution of the 4 cases. Comparing case 1, the original flexure, to case 2, the DiamondFlex with original main flexure thickness, it may be observed that the maximal stress in the system drops by 19%. Interestingly, the lateral support stiffness (y-direction) at full deflection is increased by 30 % by the adding the DiamondFlex. This may be explained by the coupling of lateral forces to the torsional motion at larger deflections. Therefore, increasing the torsional stiffness by the FLSs also increases the lateral stiffness of the PFG. The vertical support stiffness (z-direction) is unchanged.

By increasing the main flexure thickness by 28 % (case 3), the maximum stress is brought back to its limit value while the lateral support stiffness is increased by 105% at full deflection. The vertical support stiffness is increased by 42 %. Please note that the stress maximum is now located at the FLSs and not the main flexures. This shows that the theoretical maximum thickness of the main flexures is not yet obtained.

Adding a second DiamondFlex (case 4) lowers the load in the DiamondFlex, such that the main flexure can be made thicker by 44% leading to a 232 % increase of support stiffness 155% (k_{yy}) and 67% (k_{zz}), compared to the original case.

The actuation stiffness also substantially rises by the addition of the DiamondFlex elements and increased flexure thickness.

4. Discussion

4.1 Scope

The results confirm that the DiamondFlex increases the allowable thickness of the main support flexure by making the stresses uniform. This in turn allows for a higher support stiffness of the mechanism. Here, the theoretical maximum of 50 % increased main flexure thickness (Eq. 5) was almost reached when using a double DiamondFlex.

This constant curvature approach appears to work for a limited range of load and deformation cases. The main limitation lies in the stresses that are induced in the FLSs. These stresses can become quite large when large deformations are applied to the FLSs. Moreover, as actuation stiffness of main flexure strongly affects the stress in the FLSs, this approach is only satisfactory when the main flexure is relatively thin.

Furthermore, to minimize the twist angle of the FLSs, the DiamondFlex should be rather wide. Here we used a 1:1 ratio

Table 2. The performance for the parallel flexure guide without and with the DiamondFlex.

Cases		Thickness main flexure t_m $[mm]$	Width DiamondFlex w_d $[mm]$	Maximum stress $\sigma_{\max}$ [MPa]	Actuation stiffness k_{xx} [N/mm]	Support stiffness k_{yy} [N/mm]	Support stiffness k_{zz} [N/mm]
1) PFG original	$(t_\mathrm{m} = t_0)$	1.11	–	350	28.9	22.6×10^3	172×10^3
2) PFG + DiamondFlex	$(t_\mathrm{m} = t_0)$	1.11	25.5	282	44.2	29.3×10^3	172×10^3
3) PFG + DiamondFlex	$(t_\mathrm{m} > t_0)$	1.42	25.5	350	86.3	46.3×10^3	244×10^3
4) PFG + Double Diamond	$(t_\mathrm{m} > t_0)$	1.61	27.5	350	133	57.7×10^3	288×10^3

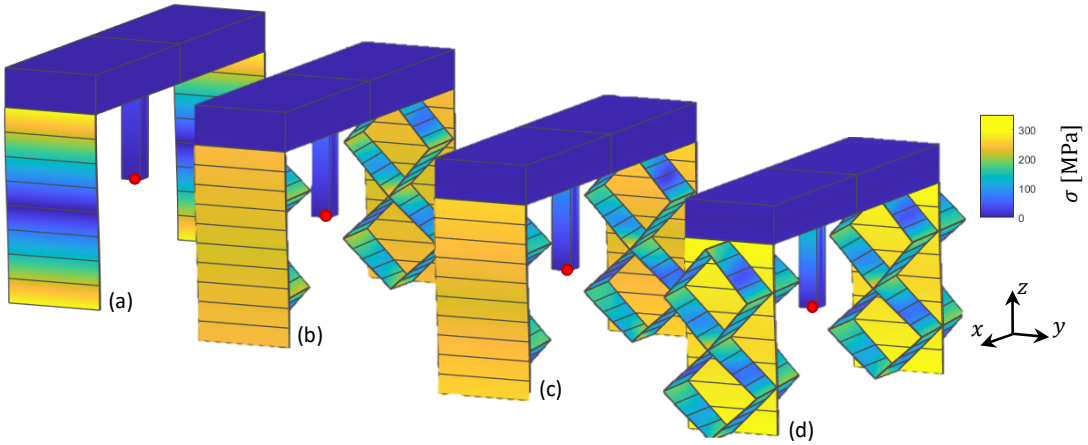

Figure 4. Deflection of a parallel flexure guide (PFG) cause stress concentrations at the fixtures *(a)*. By adding a DiamondFlex structure, these stresses are lowered and made uniform *(b)*. This allows for an increase in thickness - and hence support - without exceeding the stress limits *(c)*. A further increase in support stiffness is obtained by adding more DiamondFlex elements. The red dot indicates the force application and stiffness evaluation point.

between the breadth and its height. For a slender build volume, the twist angles become large, inducing large stresses in the FLSs

It should also be noted that this approach leads to large actuation forces as this is proportional to the cube of to the flexure thickness. Also, the added DiamondFlex increase the actuation force significantly. Potentially, this negative effect could be counteracted by statically balancing the mechanism.

4.2 Design considerations

As indicated the earlier, avoiding stress build-up in in the FLS's is crucial as this will allow for higher actuation force and a thicker main flexure. As a sufficient accurate model of the stress and support stiffness is not available at the moment, we discuss the influence of design parameters based on heuristics and experience.

Minimal producible thickness t_{d} is typically chosen for the FLSs as stress due to torsion and bending is dominant over the stress due to loading. However, very thin FLSs are prone to buckling due to this loading, placing a lower limit on the leaf spring thickness.

To minimize stress due to twisting, the FLS width w_{d} should be minimized, however this again also leads to a reduced load carrying capacity. This parameter therefore depends strongly on selected material and desired displacement of the DiamondFlex. An increased width w_d also leads to larger footprint which might not be available in all cases.

The distance to main flexure d should be as small as possible to avoid large stress due to bending while still avoiding interference. Here Equation 7 is used as a lower bound on d.

To reduce stress in the FLSs the diamond breadth b is selected to be as large as permitted by the design space. Typically, this is the same as the width of the main flexure.

There appear to be two design options for the height h of the DiamondFlex. Either the full length l_{m} of the main flexure is utilized or the height is made as small as possible to reduce the effect of bending on the stress build-up. In this paper we used the former option.

A future parameters study and analytic model would detail the limits and advantages of the presented constant curvature approach.

5. Conclusion

To conclude, this paper proposes a constant curvature flexure mechanism termed the DiamondFlex to mitigate stress concentrations that occur when flexures are subjected to an end force. The DiamondFlex consists of mirror symmetrically arranged folded leaf springs that carry the out-of-plane load. The initial 'main' flexure is therefore only loaded by a bending moment, resulting in a constant stress over its lengths. This allows the use of a thicker flexure that has a better support stiffness and load carrying capabilities.

A set of design guidelines is presented to avoid interference between the main leaf spring and the folded leaf springs and to limit the stress concentrations in the folded leaf springs.

The proposed DiamondFlex is applied to a parallel flexure guidance. Consequently, the flexures could be made thicker by 28% leading to an approximate doubling of the support stiffness. Adding another DiamondFlex in parallel allowed an even further increase in thickness by 45% and 2.5 times the original support stiffness at full deflection.

6. References

[1] S. T. Smith, *Flexures: Elements of Elastic Mechanisms*. Taylor & Francis, 2000.

[2] S. T. Smith, V. G. Badami, J. S. Dale, and Y. Xu, "Elliptical flexure hinges," *Rev. Sci. Instruments*, vol. 68, p. 1474, 1997, doi: https://doi.org/10.1063/1.1147635.

[3] S. Linß, P. Gräser, T. Räder, S. Henning, R. Theska, and L. Zentner, "Influence of geometric scaling on the elasto-kinematic properties of flexure hinges and compliant mechanisms," *Mech. Mach. Theory*, vol. 125, pp. 220–239, 2018, doi: 10.1016/j.mechmachtheory.2018.03.008.

[4] K. Dwarshuis, R. Aarts, M. Ellenbroek, and D. Brouwer, "A non-prismatic beam element for the optimization of flexure mechanisms," *Proc. ASME Des. Eng. Tech. Conf.*, vol. 2, pp. 1–10, 2020, doi: 10.1115/DETC2020-22242.

[5] J. Rommers and J. L. Herder, "Design of a Folded Leaf Spring with high support stiffness at large displacements using the Inverse Finite Element Method J.," 2019, vol. 73, pp. 2611–2620, doi: 10.1007/978-3-030-20131-9.

[6] M. Naves, D. M. Brouwer, and R. G. K. M. Aarts, "Building block-based spatial topology synthesis method for large-stroke flexure hinges," *J. Mech. Robot.*, vol. 9, no. 4, pp. 1–9, 2017, doi: 10.1115/1.4036223.

[7] J. Jonker and J. Meijaard, "SPACAR—Computer program for dynamic analysis of flexible spatial mechanisms and manipulators," in *Multibody systems handbook*, Springer, 1990, pp. 123–143.